










## The effect of deposition technique on formation of transparent conductive coatings of SnO<sub>2</sub>

E. A. Dmitrieva<sup>1</sup> , I. A. Lebedev<sup>1</sup> , E. A. Grushevskaya<sup>1</sup> , D. O. Murzalinov<sup>1</sup> ,  
A. I. Fedosimova<sup>1</sup> , A. E. Kemelbekova<sup>1\*</sup> , Zh.Sh. Kazhiev<sup>1</sup> ,  
Zh.K. Zhaysanbayev<sup>2</sup>  and A. T. Temiraliyev<sup>1</sup> 

<sup>1</sup>Satbayev University, Institute of Physics and Technology, Almaty, Kazakhstan

<sup>2</sup>Border Academy of National Security Committee of the Republic of Kazakhstan, Almaty, Kazakhstan

\*e-mail: a.kemelbekova@mail.ru

(Received 17 March 2022; received in revised form 20 April; accepted 10 May 2022)

The producing technology of transparent conductive layers is the basis for many optoelectronic devices. To increase transparency and conductivity at low-cost and controlled methods is an important challenge. Studied samples of SnO<sub>2</sub> coatings were obtained by sol-gel method. The deposition of films on glass substrates was carried out by dip coating, spin-coating and sprays-pyrolysis methods. According to micro-weighing, the film thickness varies from 250 nm to 290 nm. The layer with the most uniform thickness was achieved using spray pyrolysis. Films deposited by this technique exhibit the greatest transparency and lowest resistance. It is important to note that these samples have the minimum scatter of resistance values depending on the surface area. In case dip coating technique the resultant film contains open- and closed-type blisters. This confirms the fact of inhomogeneous surface morphology of these films. X-ray diffraction analysis showed that films obtained by spin-coating and dipping methods contain SnO<sub>2</sub> crystallites, the size of which does not exceed 10.3 nm; while films obtained by spray pyrolysis are amorphous. This is because the formation of the structure in the spray pyrolysis proceeds faster due to the substrate heating.

**Key words:** thin films, SnO<sub>2</sub>, sol-gel method, spray pyrolysis, spin-coating, dip coating, transparency, structure, resistance.

**PACS numbers:** 61.43.Dq, 39.30.+w.

### 1 Introduction

Films based on tin dioxide have a wide range of applications. For example, they are used as a sensitive element in gas analyzers. A transmittance of more than 80% over a wide wavelength range and low resistance make SnO<sub>2</sub> attractive for the production of transparent conductive coatings. The ability of the lattice oxygen to participate in chemical reaction and, at by its end, to be renewed by the oxygen from the gas phase, allows to use SnO<sub>2</sub> as a catalyst for oxidation processes. Tantalum-doped SnO<sub>2</sub> serves as capacitor electrodes in next-generation dynamic random access memory (DRAM) [1-8].

The properties of tin oxide films depend on surface homogeneity, stoichiometry, adhesion to the surface of the substrate, and other parameters. The dominant mechanism of the formation of spatial structures is

self-organization, a significant contribution to which is made by doping additives [9-12]. At the same time, the preparation method (magnetron sputtering, sol-gel method, etc.) has a significant effect on the formation of the films.

In this work, films were obtained by the sol-gel method. Due to the mild conditions of solution chemistry, this method ensures the formation of the SnO<sub>2</sub> compound without the appearance of other tin oxides in the films [13].

The method of films applying to a substrate, as a part of the producing process of investigated sample and a device based on it, effects on quality and cost. Quality, in particular, is associated with the application of a coating uniform in thickness, as well as its purity. An important aspect is the speed and controllability of the coating applying process. In sol-gel technology, there are three methods for applying

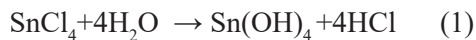
films - dipping, spin-coating and spray pyrolysis. These methods are low cost, due to do not involve complex equipment and simple in use.

The work advantage is a comprehensive analysis of SnO<sub>2</sub> films which synthesized by the sol-gel method and deposited by various methods to obtain coatings with increased transparency and surface conductivity.

## 2 Materials and Methods

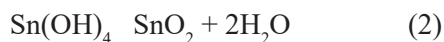
Tin oxide films were obtained from the SnCl<sub>4</sub>/EtOH film-forming system with a tin ion concentration of 0.11 mol/L. The formation of a sol and its transition into a gel occurred on the surface of the substrate.

When a film-forming system is applied to a substrate, tin tetrachloride reacts with water (from air, 3-3.5% in ethanol and 5 mol of H<sub>2</sub>O per 1 mol of SnCl<sub>4</sub> in tin tetrachloride crystalline hydrate) with the formation of a tin hydroxide sol and hydrochloric acid.



Evaporation of the solvent and reaction by-products leads to the interaction between the sol particles and the formation of a gel in which the solvent molecules are enclosed in a flexible, but sufficiently stable three-dimensional network formed by tin hydroxide particles.

Heating to 400°C promotes the removal of hydrochloric acid and solvent. As a result of this, Sn(OH)<sub>4</sub> decomposes to form water and the desired tin oxide by the reaction:



As a result, a thin film of tin (IV) oxide is formed on the surface of the substrate. The surface tension was determined by the stalagmometric method. At the next step we consider each way of the film deposition in detail.

**Dip coating technique.** A film-forming system was applied on one side of the glass substrate, dried for 1-2 minutes and then annealed in air at 400°C for 15 minutes.

**Spin coating technique.** A film-forming system was applied to a substrate mounted on a spinner. Rotation speed - 3000 rpm, time - 3 seconds. Then the samples were dried with an infrared emitter from

room temperature to 80°C for 1 minute. At the final stage, the samples were annealed in a muffle furnace at  $t = 400^\circ\text{C}$  for 15 minutes.

**Spray pyrolysis technique.** A film-forming system was sprayed at a pressure of 1.8 atm onto a substrate heated to 400°C.

In all cases 15 layers were deposited.

The film thickness was determined by micro-weighing. When calculating the thickness of the films, the following formula was used:

$$d = (m_{\text{sample}} - m_{\text{substrate}}) / (\rho_{\text{(tin oxide)}} * S_{\text{substrate}}) \quad (3)$$

where:

$d$  – film thickness;

$m_{\text{sample}}$  – mass of the sample;

$m_{\text{substrate}}$  – mass of the glass substrate;

$\rho_{\text{tin}}$  – oxide is the density of cassiterite taken as 7 g/cm<sup>3</sup>;

$S_{\text{substrate}}$  – area of the glass substrate.

## 3 Results and Discussion

The transmission spectra were measured on a UNICO SpectroQuest 2800 spectrophotometer. The morphology of the films was studied using a JSM-6490LA, JEOL scanning electron microscope. The structure of the films was determined using x-ray diffraction analysis on a DRON-6 diffractometer.

Table 1 shows the thicknesses of the films calculated by the micro-weighing method.

**Table 1** – Film thickness calculated from micro-weighing measurement

Deposition technique	Thickness, nm
Dip coating	270±14
Spin coating	250±14
Spray pyrolysis	290±14

From the Table 1 it is seen that the thickness of the films varies from 250 nm to 290 nm. It is assumed that the film is uniformly distributed over the surface of the substrate and has the density of a natural SnO<sub>2</sub> crystal (cassiterite).

Figure 1 shows the distribution of forces acting on the film-forming system, depending on the deposition method.

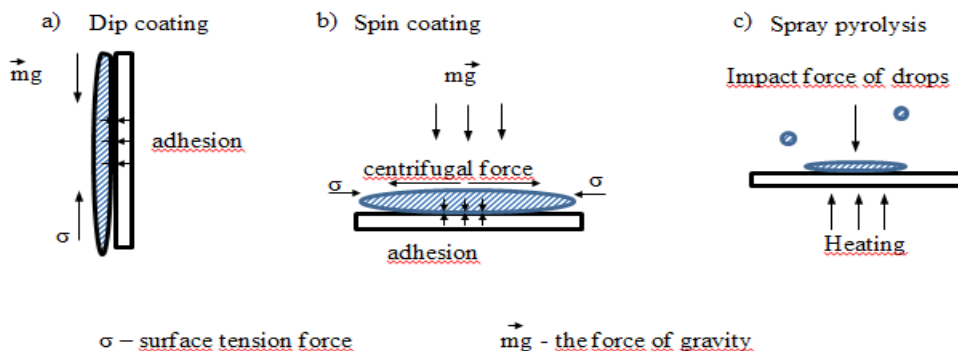


**Figure 1** – Scheme of the distribution of forces depending on the deposition technique

As can be seen from Figure 1a, when a film-forming system is applying by dipping, the force of gravity, the adhesion force to the substrate surface and the surface tension force act on the  $\text{SnCl}_4/\text{EtOH}$  system. The net force tends to gather the fluid into the sphere.

In this case, adhesion causes a bonding between the solid substrate and the fluid contacting with it. Wetting is the result of such a bond. The Dupre-Young equation [14-15] shows the relationship between adhesion and wetting:

$$W_a = \sigma_{12} (1 + \cos \theta) \quad (4)$$

where  $\sigma_{12}$  is a surface tension at the interface between two phases (liquid-gas);  $\theta$  is a contact angle;  $W_a$  is a reversible work of adhesion.

The surface tension of the film-forming system =  $21.8 \cdot 10^3$  N/m, the contact angle in the system “glass substrate / film-forming system” ( $\theta$ ) tends to zero. Then  $W_a \approx 43.6 \cdot 10^3$  N/m.

On the lower part of a vertically arranged substrate, there is a formation of a liquid drop that is balanced by gravity and surface tension. At this, on the upper part of the sample, the evaporation of the solvent and the course of reaction (1) lead to the formation of solid phase of  $\text{Sn}(\text{OH})_4$  (sol) and its structuring (gel). Removing a drop of a film-forming solution from a sample, we take a portion of the liquid mass, thereby disturbing the force balance. Now the forces of surface tension prevail, and the film-forming system moves up until the force balance is reached. At this time, the film thickness increases in this place. Further annealing fixes the obtained film on the substrate. Thus, in case of dip coating technique, the film has a thickness variation in different parts of the sample.

During spin-coating deposition (Fig. 1b), such forces as adhesion, surface tension and centrifugal force act on the film-forming system. The speed and time of rotation were selected experimentally based on the fact that the surface should be smooth. Under the action of centrifugal forces, part of the film-forming system “flies away” from the surface of the substrate. There is a formation of a thin layer, which, after the rotation stop, begins to pull toward the center from the substrate edges under the action of surface tension. There might be a fracture formation due to small surface defects, which breaks the film integrity. To fix the layer, the film was heated by an infrared emitter immediately after the rotation stop and then annealed.

Films obtained by spin coating are more uniform in thickness, in contrast to films prepared by dipping technique. However, the interference pattern is observed along the edge of substrate at a distance of about 0.5 cm. This indicates the thickness inhomogeneity of the film.

Deposition by spray pyrolysis (Fig. 1c) takes place on a hot substrate. The film-forming system is supplied under pressure. The main role is played by the size and sedimentation rate of the droplets. Contact with a hot substrate leads to evaporation of the solvent and the course of reactions (1) and (2).

In this case, the interference pattern was not observed on the obtained samples. This indicates a more uniform layer thickness.

### 3.1 Surface morphology

Analysis of the surface morphology of obtained samples using electron microscopy showed that the films prepared by dip coating contain blisters, depicted in Figure 1.

The figure on the left shows open- and closed-type blisters; the right image shows the sizes of the open blister.

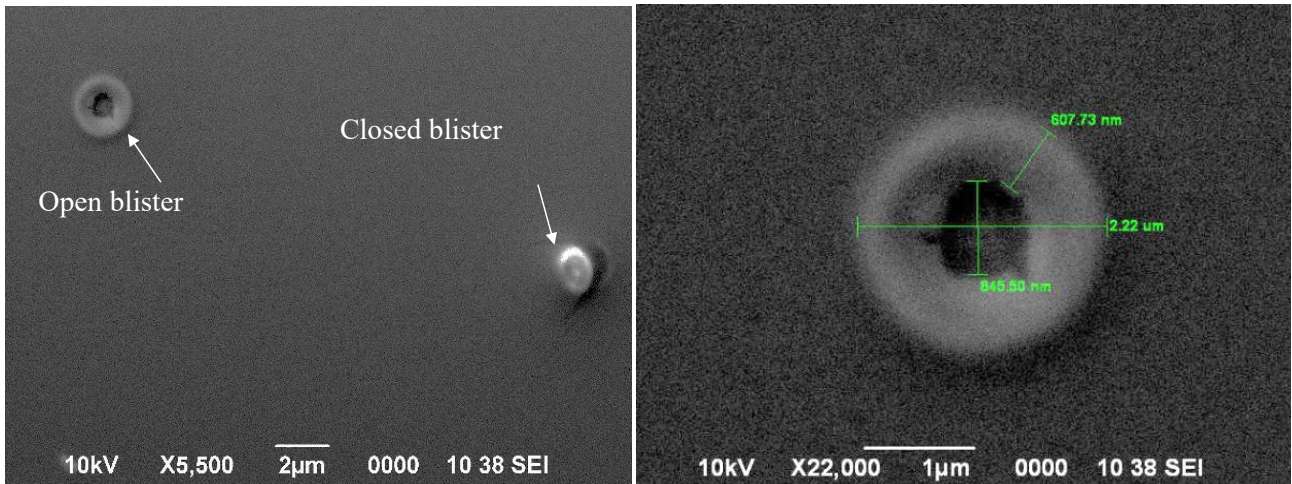


Figure 2 – Blisters on the surface of a film deposited by dip coating technique.

In this work, multilayer films were obtained. Each layer was annealed at 400°C. The deposition of layers on a substrate that not cooled down completely (the temperature of the each layer is not exceed 60°C), leads to the formation of solvent vapors and reaction products at the “film – substrate” interface. The vapors “lift” an unhardened film. Thus,

blisters are formed when a film-forming system is applied to a heated surface. As a result, the films demonstrate inhomogeneous surface morphology [16-18].

3.2 Optical properties

Figure 3 shows the transmission spectra of thin SnO<sub>2</sub> films deposited by different techniques.

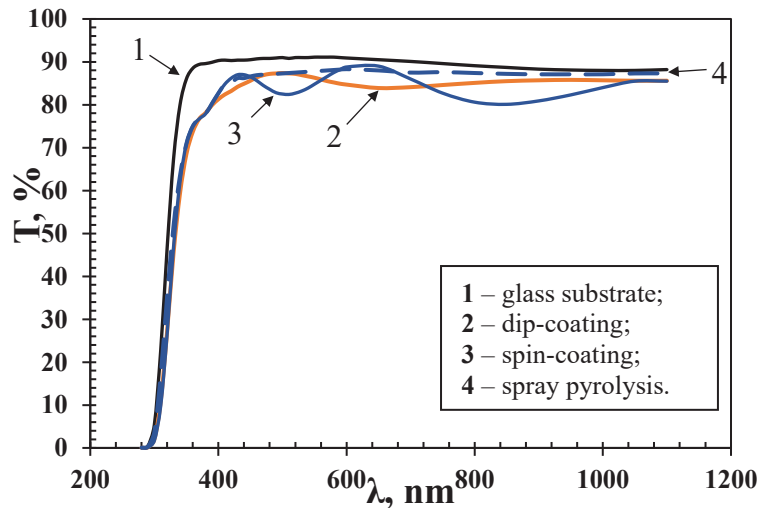


Figure 3 – Transmission spectra of films prepared by different methods

As can be seen from Figure 3, films deposited by different methods have a transmittance of more than 80% in the range  $\lambda = 380-1100$  nm. This makes them attractive as transparent coatings. On the spectra of films deposited by spin coating and dip

coating, interference peaks are observed. There are no interference peaks in the transmission spectrum of a film deposited by the pyrolysis spray method. The value of transmittance of the film deposited by the pyrolysis spray method is the highest and is more



than 86% in the wavelength range from 440nm to 1100nm.

Based on the available interference peaks, the parameters of the films were calculated using the envelope method [19]. The results of the calculation are shown in table 2.

**Table 2** – Film parameters calculated from interference peaks

	Dip coating	Spin coating
Film thickness, nm	296	375
Extinction coefficient	$11.0 \cdot 10^{-3}$	$8.1 \cdot 10^{-3}$
Refraction index	1.689	1.722
Absorption coefficient	$2.89 \cdot 10^3$	$3.37 \cdot 10^3$

From table 2 it is seen that the thickness of the films calculated from the transmission spectra is greater than the thickness calculated by the micro-weighing method. This discrepancy is due to the difference between the density of the films and the density of cassiterite. Thus, the film deposited by spin coating is less dense than the film deposited by dipping.

### 3.3 Electrical resistance of the films

The resistance of the films was determined by 10 measurements in different parts of the samples. The distance between the contacts is 1 mm. Student's coefficient for 10 measurements with a reliability of  $0.95 = 2.262$ . The error was calculated by the formula:

$$\Delta \bar{A} = t_{\gamma, n-1} \sqrt{\frac{\sum_{i=1}^n (A_i - \bar{A})^2}{\frac{n-1}{\sqrt{n}}}} \quad (5)$$

where  $\Delta \bar{A}$  is an absolute error;  $t_{\gamma, n-1}$  is a Student's coefficient;  $A_i$  is a value of the  $i$ -th measurement;  $\bar{A}$  is an arithmetic mean value,  $n$  is the number of measurements.

**Table 3** – The average values of the active resistance of the films

Deposition technique	Resistance
Dip coating	$198 \pm 29 \text{ k}\Omega$
Spin coating	$193.5 \pm 16.6 \text{ k}\Omega$
Spray pyrolysis	$13.3 \pm 0.8 \text{ k}\Omega$

From the Table 3 it is seen that the resistance of the films deposited by dip- and spin-coating are close. The resistivity of films deposited by spray pyrolysis is much lower and equals to  $13.3 \pm 0.8 \text{ k}\Omega$ .

The scatter of values over the sample surface is noteworthy. The fluctuation of the resistance value depending on the surface area equals to  $\pm 29 \text{ k}\Omega$  (14.6%),  $\pm 16.6 \text{ k}\Omega$  (8.6%) and  $\pm 0.8 \text{ k}\Omega$  (6.0%) for the films deposited by dip coating, spin coating and spray pyrolysis, respectively. Films deposited by spray pyrolysis have a lower resistance and a smaller scatter of values depending on the surface area. This makes them more attractive for use as conductive coatings.

### 3.4 X-ray diffraction analysis

Tin oxide signal in raw XRD spectra was weakly expressed as the halo from the glass substrate prevailed. Using the method that allows to increase the signal-to-noise ratio [20], the following data were obtained and analyzed. Figure 4 shows the results of X-ray diffraction analysis of  $\text{SnO}_2$  films.

Figure 4 show the films obtained by spray pyrolysis are amorphous. Films obtained by spin coating and dipping method contain  $\text{SnO}_2$  crystallites.

The average crystallite size ( $D$ ) of the synthesized samples was estimated by X-ray line broadening according to the Scherrer formula [21]:

$$D = (k\lambda / (\beta \cos\theta)) \quad (6)$$

where  $k$  is a Scherrer constant, usually taken as 0.9, but its value strongly depends on the crystallite shape [22];  $\lambda$  is X-ray wavelength;  $\theta$  is a Bragg diffraction angle;  $\beta$  is a line broadening at half the maximum intensity (in rad).

The measurement accuracy was calculated from the broadening of the diffraction line  $\Delta\beta = 0.1 \text{ rad}$ . The results of the calculation of crystallite sizes are shown in Table 4.

Table 4 shows that  $\text{SnO}_2$  films deposited by dip coating and spin coating are nanocrystalline. The crystallite size does not exceed 10.3 nm.

The formation of the amorphous structure of the films obtained by spray pyrolysis is probably associated with the high rate of reactions (1) and (2), since deposition occurs on a heated substrate. Consequently, crystallite formation will occur with further increase in the duration and temperature of annealing.

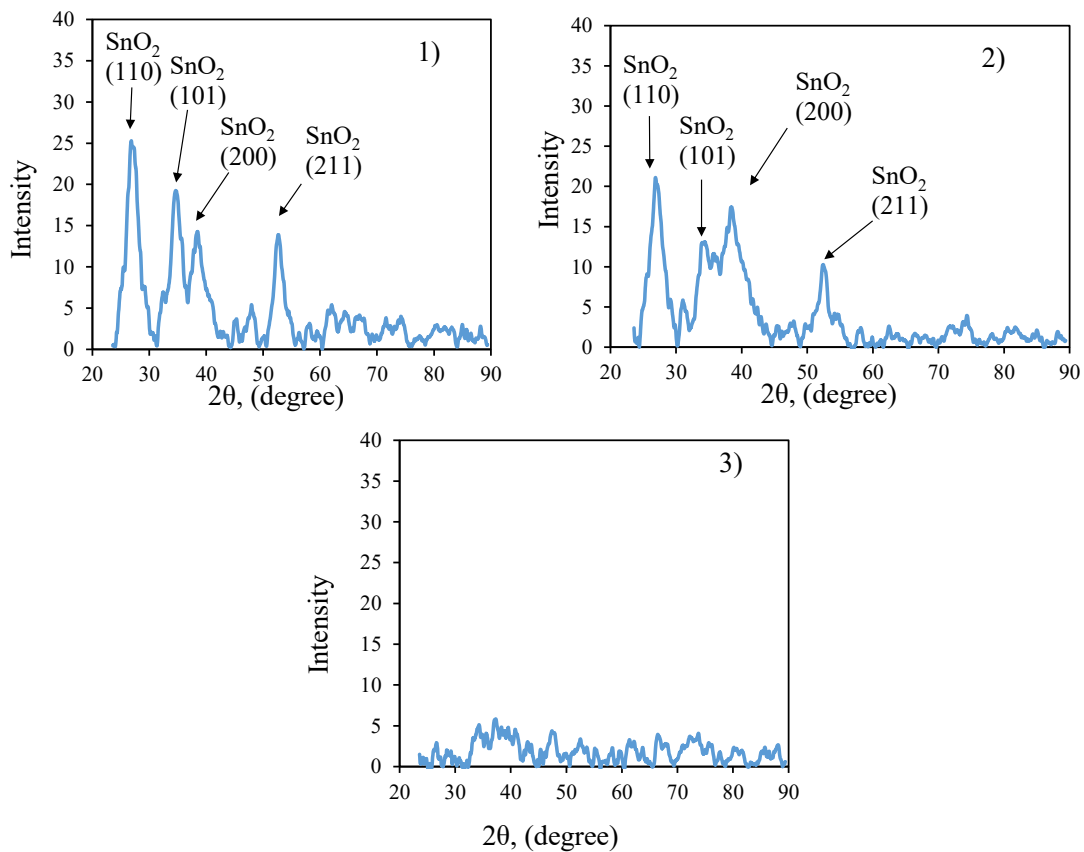


**Figure 4** – X-ray diffraction pattern of films deposited by different techniques (1 – dip coating, 2 – spin coating, 3 – spray pyrolysis)

**Table 4** – Sizes of SnO<sub>2</sub> crystallites

Deposition technique	SnO <sub>2</sub>			
	(110)	(101)	(200)	(211)
Dip coating	6.2±0.2 nm	6.6±0.2 nm	7.7±0.2 nm	9.1±0.3 nm
Spin coating	6.5±0.2 nm	5.2±0.2 nm	4.6±0.2 nm	10.3±0.3 nm

#### 4 Conclusions

Visual inspection and SEM analysis showed that films deposited by spray pyrolysis technique demonstrate the best surface morphology and thickness uniformity, comparing to films formed by dip coating technique that contain blisters, and spin coated films having interference patterns on the edges.

Films deposited by all three different methods have a transmittance of more than 80% in the range of 380-1100 nm. However, the highest transmittance of 86%, and the minimum electrical resistance were observed in the films deposited by spray pyrolysis. Moreover, the films obtained by this method dem-

onstrate the highest sheet resistance uniformity (with the value scatter of 6%). These qualitative advantages make spray pyrolysis deposition technique the effective and optimal method for creating transparent conductive coatings based on tin dioxide.

XRD analysis revealed that dip coating and spin coating deposition techniques form nanocrystalline SnO<sub>2</sub> films, with the crystallite size of 10.3 nm and less. Films deposited by spray pyrolysis have an amorphous structure. This explained by the high rate of sol-gel processes on heated substrate. The process of the crystallites formation in this method can be controlled by increasing the duration and temperature of annealing.

## Acknowledgments

This research was funded the program № AP09058002 «Investigation of the properties of dynamic memory based on Si<sub>3</sub>N<sub>4</sub>/Si

and the formation of silicon nanoclusters with increased photoluminescence intensity» by the Committee of Science of the Ministry of Education and Science of the Republic of Kazakhstan.

## References

1. E.A. Dmitriyeva, D.M. Mukhamedshina, K.A. Mit', I.A. Lebedev, I.I. Girina, A.I. Fedosimova, E.A. Grushevskaya. Doping of fluorine of tin dioxide films synthesized by sol-gel method // News of the National Academy of Sciences of the Republic of Kazakhstan (series of geology and technical sciences). – 2019. – Vol.433. – P.73-79. <https://doi.org/10.32014/2019.2518-170X.9>.
2. E.A. Grushevskaya, S.A. Ibraimova, E.A. Dmitriyeva, I.A. Lebedev, K.A. Mit', D.M. Mukhamedshina., A.I. Fedosimova, A.S. Serikkanov, A.T. Temiraliyev. Sensitivity to ethanol vapour of thin films SnO<sub>2</sub> doped with fluorine // Eurasian Chemico Technological J. – 2019. – Vol.21. – P.13-17. <https://doi.org/10.18321/ectj781>.
3. H.F. Guo, Z.W. Chen, X. Wang, Q.F. Cang, C.H. Ma, X.G. Jia, N.Y. Yuan, J.N. Ding. Significant increase in efficiency and limited toxicity of a solar cell based on Sb<sub>2</sub>Se<sub>3</sub> with SnO<sub>2</sub> as a buffer layer // Journal of Materials Chemistry C. – 2019. – Vol. 7(45). – P. 14350-14356, <https://doi.org/10.1039/c9tc04169a>.
4. D. Wang, S.C. Chen, Q.D. Zheng. Poly(vinylpyrrolidone)-doped SnO<sub>2</sub> as an electron transport layer for perovskite solar cells with improved performance // Journal of Materials Chemistry C. – 2019. – Vol.7 (39). – P. 12204-12210. <https://doi.org/10.1039/c9tc04269e>.
5. B. Matthias, D. Ulrike. The surface and materials science of tin oxide // Progress in Surface Science. – 2005. – Vol. 79. – P. 47-154. <https://doi.org/10.1016/j.progsurf.2005.09.002>.
6. R.Y. Zhang, F.F. Zhu, Y. Dong, X.M. Wu, Y.H. Sun, D.R. Zhang, T. Zhang, M.L. Han. Function promotion of SO<sub>4</sub><sup>2-</sup>/Al<sub>2</sub>O<sub>3</sub>-SnO<sub>2</sub> catalyst for biodiesel production from sewage sludge // Renewable energy. – 2020. – Vol. 147. – P. 275-283. <https://doi.org/10.1016/j.renene.2019.08.141>.
7. Z. Chen, T.T. Fan, Y.Q. Zhang, J. Xiao, M.R. Gao, N.Q. Duan et al. SnO<sub>2</sub> catalyzed simultaneous reinforcement of carbon dioxide adsorption and activation towards electrochemical conversion of CO<sub>2</sub> to HCOOH // Applied catalysis b-environmental. – 2020. – Vol. 261. – P. 118243-118249. <https://doi.org/10.1016/j.apcatb.2019.118243>.
8. B.H. Zhang, L.Z. Sun, Y.Q. Wang, Chen S., J.T. Zhang. Well-dispersed SnO<sub>2</sub> nanocrystals on N-doped carbon nanowires as efficient electrocatalysts for carbon dioxide reduction // Journal of energy chemistry. – 2020. – Vol. 41. – P. 7-14. <https://doi.org/10.1016/j.jechem.2019.04.022>.
9. C.J. Cho, M.S. Noh, W.C. Lee, C.H. An, C.Y. Kang, C.S. Hwang, S.K. Kim. Ta-doped SnO<sub>2</sub> as a Reduction-Resistant Oxide Electrode for DRAM Capacitors // Journal of Materials Chemistry C. – 2017. – Vol. 5(36). – P. 9405-9411. <https://doi.org/10.1039/c7tc03467a>.
10. A.I. Fedosimova, E.A. Dmitrieva, I.A. Lebedev, A.T. Temiraliyev, M.E. Abishev, B.A. Baitimbetova, Yu.A. Ryabikin, A.S. Serikkanov. Modeling the process of formation of fractal structures in thin films // IOP Conf. Series: Journal of Physics: Conf. Series. – 2018. – Vol. 1141, Id. 012004. – P. 1-7. <https://doi.org/10.1088/1742-6596/1141/1/012004>.
11. D.M. Mukhamedshina, A.I. Fedosimova, E.A. Dmitriyeva, I.A. Lebedev, E.A. Grushevskaya, S.A. Ibraimova, K.A. Mit', A.S. Serikkanov. Influence of plasma treatment on physical properties of thin SnO<sub>2</sub> films obtained from SnCl<sub>4</sub> solutions with additions of NH<sub>4</sub>F and NH<sub>4</sub>OH // Eurasian Chemico-Technological Journal. – 2019. – Vol.21(1). – P.57-61. <https://doi.org/10.18321/ectj791>.
12. E.A. Dmitrieva, D.M. Mukhamedshina, N.B. Beisenkhanov, K.A. Mit'. The effect of NH<sub>4</sub>F and NH<sub>4</sub>OH on the structure and physical properties of thin SnO<sub>2</sub> films synthesized by the sol-gel method // Glass Physics and Chemistry. – 2014. – Vol.40. – No1. – P. 31-36. – <https://doi.org/10.1134/S1087659614010076>.
13. J.W. Drelich, L. Boinovich, E. Chibowski, C. Della Volpe, L. Holysz, A. Marmur, S. Siboni. Contact angles: History of over 200 years of open questions // Surface Innovations. – 2020. – Vol. 8(1-2). –P. 3-27. <https://doi.org/10.1680/jsuin.19.00007>.
14. T. Guo, J.Y. He, X.L. Pang, A.A. Volinsky, Y.J. Su, L.J. Qiao. High temperature brittle film adhesion measured from annealing-induced circular blisters // Acta materialia. – 2017. – Vol. 138. – P.1-9. <https://doi.org/10.1016/j.actamat.2017.07.026>.
15. I.A. Karapatnitski, K.A. Mit', D.M. Mukhamedshina, N.B. Beisenkhanov. Optical, structural and electrical properties of tin oxide films prepared by magnetron sputtering // Surface and Coat.Technol.. – 2002. – Vol. 151 – 152. – P. 76 – 81.

16. F.K. Konan, B. Hartiti, A. Batan, B. Aka. X-ray diffraction, XPS, and Raman spectroscopy of coated ZnO:Al (1–7 at%) // nanoparticles // E-Journal of Surface Science and Nanotechnology. –2019. –Vol. 17. P. 163-168. <https://doi.org/10.1380/ejsnt.2019.163>.
17. F.K. Konan, J.S. Ncho, H.J.T. Nkuissi, B. Hartiti, A. Boko. Influence of the precursor concentration on the morphological and structural properties of zinc oxide (ZnO) // Materials Chemistry and Physics. – 2019. – Vol.229. – P. 330-333. <https://doi.org/10.1016/j.matchemphys.2018.12.082>.
18. N.M. Tompakova, E.A. Dmitrieva, E.A. Grushevskaya, I.A. Lebedev, A.S. Serikkanov, D.M. Mukhamedshina, K.A. Mit. The effect of three-minute hydrogen plasma treatment on the structure and properties of SnO<sub>2</sub> thin films //Recent Contributions to Physics. – 2019. – № 4(71). – P. 67–74. <https://doi.org/10.26577/RCPH-2019-i4-9>. (in Russian)
19. N. K. Mishra, Ch.Kumar, A. Kumar, M. Kumar, P. Chaudhary, R. Singh. Structural and optical properties of SnO<sub>2</sub>-Al<sub>2</sub>O<sub>3</sub> nanocomposite synthesized via sol-gel route //Materials Science-Poland. – 2015. – Vol. 33(4). – P.714-718. <https://doi.org/10.1515/msp-2015-0101>.
20. D.M. Mukhamedshina, N.B. Beisenkhanov, K.A. Mit', V.A. Botvin, I.V. Valitova, E.A. Dmitrieva. Influence of plasma treatments on the properties of SnOx thin films //High Temperature Material Processes. – 2006. – Vol. 10(4). – P. 603-615. <https://doi.org/10.1615/HighTempMatProc.v10.i4.110>.
21. S.-K.Song. Color-octet mechanism in  $\gamma^+ \rightarrow pJ/\psi + X$  // Phys. Rev. – 1999. –Vol. 60. –. P. 11137 – 11148.
22. B.N. Mukashev, A.B. Aimagambetov, D.M. Mukhamedshina, N.B. Beisenkhanov, K.A. Mit, I.V. Valitova, E.A. Dmitrieva. Study of structural, optical and electrical properties of ZnO and SnO<sub>2</sub> thin films // Superlattices and Microstructures. – 2007. – Vol. 42(1-6). – P. 103-109. <https://doi.org/10.1016/j.spmi.2007.04.057>.

© This is an open access article under the (CC)BY-NC license (<https://creativecommons.org/licenses/bync/4.0/>).  
Funded by Al-Farabi KazNU